



Determinants of Treatment Response in Painful Diabetic Peripheral Neuropathy: A Combined Deep Sensory Phenotyping and Multimodal Brain MRI Study

Iain David Wilkinson,¹ Kevin Teh,¹ Francesa Heiberg-Gibbons,² Mohammad Awadh,² Alan Kelsall,³ Pallai Shillo,³ Gordon Sloan,³ Solomon Tesfaye,³ and Dinesh Selvarajah²

Diabetes 2020;69:1804–1814 | <https://doi.org/10.2337/db20-0029>

Painful diabetic peripheral neuropathy (DPN) is difficult to manage, as treatment response is often varied. The primary aim of this study was to examine differences in pain phenotypes between responders and nonresponders to intravenous lidocaine treatment using quantitative sensory testing. The secondary aim was to explore differences in brain structure and functional connectivity with treatment response. Forty-five consecutive patients who received intravenous lidocaine treatment for painful DPN were screened. Twenty-nine patients who met the eligibility criteria (responders, $n = 14$, and nonresponders, $n = 15$) and 26 healthy control subjects underwent detailed sensory profiling. Subjects also underwent multimodal brain MRI. A greater proportion of patients with the irritable (IR) nociceptor phenotype were responders to intravenous lidocaine treatment compared with nonresponders. The odds ratio of responding to intravenous lidocaine was 8.67 times greater (95% CI 1.4–53.8) for the IR nociceptor phenotype. Responders to intravenous lidocaine also had significantly greater mean primary somatosensory cortex cortical volume and functional connectivity between the insula cortex and the cortico-limbic circuitry. This study provides preliminary evidence for a mechanism-based approach for individualizing therapy in patients with painful DPN.

Painful distal symmetrical diabetic peripheral neuropathy (DPN) is one of the most challenging complications of diabetes to manage effectively (1). The mainstay of treatment is pharmacotherapy, but the best we can hope for is

50% pain relief in only a third of patients (2). The current approach assumes that all patients respond similarly to a given drug when in fact there is a wide variability in response. This reflects a failure to target specific pain-generating mechanisms that result from nerve injury. In response to nerve injury, damaged nerve endings undergo a series of changes (degeneration and regeneration) within the peripheral and central nervous system (CNS), which leads to sensitization. Hence, the overarching aim of this proof-of-concept study was to examine changes within the peripheral and CNS and relate these to treatment response in painful DPN. If confirmed, the prospective classification of patients according to unique features within the peripheral and/or CNS may play an increasingly important role in personalized treatment of painful DPN.

Using detailed peripheral nerve quantitative sensory testing (QST) on a large sample of patients with painful DPN, Themistocleous et al. (3) revealed a distinct range of sensory profiles that could be broadly categorized into two pain phenotypes: 1) irritable (IR) nociceptor with preserved small-fiber function together with hyperalgesia, and 2) nonirritable (NIR) nociceptor phenotype dominated by sensory loss or deafferentation. The key mechanism resulting in the IR nociceptor phenotype is understood to be ectopic activity in newly formed or upregulated sodium channels. Recent work by Demant et al. (4) found that oxcarbazepine, a compound with an ability to block sodium channels, has greater efficacy in patients with the IR compared with the NIR nociceptor phenotype. Intravenous lidocaine, another sodium channel inhibitor, can provide

¹Academic Department of Radiology, Department of Infection, Immunity and Cardiovascular Disease, University of Sheffield, Sheffield, U.K.

²Department of Oncology and Human Metabolism, University of Sheffield, Sheffield, U.K.

³Diabetes Research Department, Sheffield Teaching Hospitals NHS Foundation Trust, Sheffield, U.K.

Corresponding author: Dinesh Selvarajah, d.selvarajah@sheffield.ac.uk

Received 9 January 2020 and accepted 26 May 2020

This article contains supplementary material online at <https://doi.org/10.2337/figshare.12370478>.

I.D.W. and K.T. are joint first authors.

© 2020 by the American Diabetes Association. Readers may use this article as long as the work is properly cited, the use is educational and not for profit, and the work is not altered. More information is available at <https://www.diabetesjournals.org/content/license>.

safe and effective treatment for neuropathic pain that does not respond to standard oral agents (5–7). However, it is only effective in less than half of patients with painful DPN (8), and this could be related to its specific mechanism of action. Lidocaine exhibits state-dependent binding in which sodium channels that are rapidly and repeatedly activated and inactivated are more readily blocked (9). This state dependence limits the hyperexcitability of cells exhibiting abnormal activity. Thus, we hypothesize that intravenous lidocaine will have greater efficacy in patients with the IR nociceptor phenotype (10,11). If confirmed, this could enable future patient stratification, leading to a more efficient treatment approach. Hence, the primary aim of this study was to examine differences in sensory profiling between intravenous lidocaine responders and nonresponders in painful DPN.

Within the CNS, we recently demonstrated reduction in cortical volume and functional reorganization in the primary somatosensory cortex (S1) in patients with painful DPN with the deafferentation or painful insensate phenotype (12). This represents a more advanced painful hypoesthesia phenotype that, like the NIR nociceptor phenotype, is characterized by deafferentation or a dying-back axonopathy. Hence, using multimodal MRI of the brain, we will also explore (secondary aim) if nonresponders to intravenous lidocaine have structural and functional CNS alterations that correspond to this sensory phenotype.

RESEARCH DESIGN AND METHODS

Study Population

Forty-five consecutive patients currently attending the Royal Hallamshire Hospital (Sheffield, U.K.) for intravenous lidocaine treatment were screened. This was an open-labeled, observational cohort study. A 5 mg/kg dose of lidocaine (AstraZeneca, Westborough, MA) (in 100 mL of normal saline solution) was administered intravenously over a 60-min period. This is based on ideal body weight with maximum dose of 300 mg. The infusion was stopped if unacceptable side effects occurred (e.g., nausea, tinnitus, and arrhythmia). Three-lead electrocardiogram, heart rate, and blood pressure were monitored throughout the infusion and for 30 min thereafter.

Inclusion criteria were: type 1 or 2 diabetes diagnosed for >5 years, between 18 and 65 years of age, stable glycemic control ($HbA_{1c} < 11\%$ [97 mmol/mol]), neuropathic symptoms confirmed on Douleur Neuropathique 4 (DN4; cutoff score >4) (13), and patients who have no contraindications to receive intravenous lidocaine treatment. Exclusion criteria were: pregnancy, insufficient command of English or mental capacity to provide informed consent or to complete the study questionnaires, concurrent severe psychological/psychiatric disorders, moderate-to-severe pain from other causes that may confound assessment or reporting of pain, patients with central nervous lesions, which may complicate somatosensory testing, patients who were intolerant of intravenous lidocaine, nondiabetic neuropathies, history of alcohol consumption of >20 units/

week (1 unit is equivalent to 1 glass of wine or 1 measure of spirits), diabetic neuropathies other than DPN (e.g., mononeuropathies or proximal motor neuropathies), epilepsy, recurrent severe hypoglycemia and hypoglycemic unawareness, and other factors that would preclude MRI (e.g., pacemaker, claustrophobia, etc.). All patients underwent detailed clinical history, physical examination, and blood tests to ensure they met study inclusion and exclusion criteria.

Treatment Response

Patients were contacted by telephone 1 week after intravenous lidocaine treatment to perform efficacy assessments using a pain questionnaire. Responders were defined as patients who report at least a 30% reduction in pain intensity score (11-point numeric rating scale [NRS], in which 0 is no pain and 10 is worst pain imaginable) within a week after lidocaine treatment lasting for at least 3 weeks (14).

Out of 45 patients screened, 29 patients were invited to participate in two study visits (visit 1, neurophysiological assessments and sensory phenotyping and visit 2, MRI). Patients and investigators were aware of treatment response at screening. All study assessments were performed off all of the other neuropathic pain treatments (for a minimum of 48 h or up to five half-life) in order to avoid the possible confound of a therapeutic effect on these assessments. Paracetamol was taken as rescue medication if required. As responders are receiving treatment every 8 weeks, study assessments were performed before lidocaine treatment was administered. Twenty-six healthy volunteers (HVs) (aged 54.0 [11.9] years and 11 males [42.3%]) were also recruited to serve as control subjects and underwent assessments as per visit 1 and 2. Inclusion criteria for healthy control subjects were: no history of chronic medical conditions, not taking any regular medications, and no current or past history of chronic pain conditions. Exclusion criteria: pregnancy, insufficient command of English or mental capacity to provide informed consent or to complete the study questionnaires, concurrent severe psychological/psychiatric disorders, history of alcohol consumption of >20 units/week (1 unit is equivalent to 1 glass of wine or 1 measure of spirits), and other factors that would preclude MRI (e.g., pacemaker, claustrophobia, etc.). Written informed consent for the study was obtained before subjects participated in the study, which has prior approval by the Sheffield Local Research Ethics Committee (Sheffield, U.K.).

Sensory Phenotyping/Quantitative Sensory Assessments

QST is a means of assessing sensory phenotype, and differences in QST parameters may give insight into pathophysiological mechanisms. All patients with painful DPN underwent QST of the feet using the protocol developed by the German Research Network on Neuropathic Pain (DFNS) (15). G.S., M.A., and F.H.-G. underwent

formal training in conducting the DFNS QST protocol at the University of Mannheim using HVs. QST results were used to classify patients into IR and NIR nociceptor phenotypes. Cold and warm detection thresholds as well as cold and heat pain thresholds and thermal sensory limen (including paradoxical heat sensations) were established using a Medoc TSA 2 Neurosensory Analyzer (Medoc Advanced Medical Systems, Ramat Yishai, Israel). We also tested mechanical detection and pain thresholds, mechanical pain sensitivity, allodynia, pressure pain thresholds (PPTs), wind-up ratio (WUR), and vibration detection thresholds. Mechanical detection threshold was assessed with a set of standardized von Frey filaments (0.25, 0.5, 1, 2, 4, 8, 16, 32, 64, 128, and 256 mN [Marstock Nervtest, Marburg, Germany]) using a modified method of limits. Mechanical pain threshold was assessed with a set of seven metal probes with standardized stimulus intensities (8, 16, 32, 64, 128, 256, and 512 mN; MRC Systems GmbH Medizintechnische Systeme, Heidelberg, Germany) with a uniform skin contact area of 0.25 mm, using a modified method of limits. Mechanical pain sensitivity of the skin and dynamic mechanical allodynia were determined by the same set of seven metal probes with standardized stimulus intensities and in addition by a set of seven light-intensity stimuli: a cotton wool ball with a force of 3 mN, a Q-tip (fixed to a plastic stick) with a force of 100 mN, and a paintbrush with an applied force of between 200 and 400 mN. These stimuli were applied 50 times (5 runs of 10 stimuli per test site in different pseudorandomized sequences), and the patients were asked to rate the intensity of each stimulus on a 0–100 NRS (0 being no pain and 100 the most severe pain). WUR, as a measure of enhanced temporal summation, was examined by a pinprick stimulus with standardized intensity (256 mN). The stimulus was first applied singularly and then in a series of 10 stimuli with a frequency of 1 Hz within an area of 1 cm². Patients were asked to rate the intensity of the first and mean of 10 stimuli on a 0–100 NRS. The ratio between the two measures was calculated as WUR; a WUR of >1 indicates enhanced temporal summation. Vibration detection threshold was examined with a tuning fork (64 Hz; 8 out of 8 scale) at the (lateral or medial) malleolus area. Muscular PPT was examined by applying mechanical pressure at a 0.5 kg/s rate (Algometer; Somedic AB, Sösdala, Sweden) at the abductor hallucis muscle. Except for the vibration detection threshold and PPT, all sensory tests are performed in the S1 dermatome bilaterally (unless defined by the distribution of symptoms). Participants were familiarized with the testing procedure on the dorsum of the forearm before all parameters were measured over the dorsum of both feet (S1 dermatome). PPTs were recorded over the arch of the foot, and vibration detection thresholds were tested over the medial malleolus. QST data were entered into the data analysis system eQUISTA provided by the DFNS. eQUISTA transformed the raw QST data into z scores, thus normalizing for age, sex, and the body location of testing (16).

Definition of Sensory Phenotype

Our sensory profiling methodology and definition of sensory phenotypes were based on recent recommendations of the DFNS, Europain, and Neuropain consortia (17). IR nociceptor phenotype is the presence of dynamic mechanical allodynia, reduced mechanical or pressure threshold, increased mechanical pain sensitivity, or lower cold or heat pain threshold or any combination of these signs of hyperexcitability (17). NIR nociceptor phenotype included patients not classified as IR nociceptor phenotype (i.e., sensory loss with no signs of hyperexcitability).

Structured Neurological Examination

All patients completed the Neuropathy Total Symptom Score-6 (NTSS-6) questionnaire, which evaluates the frequency and intensity of individual neuropathy sensory symptoms (numbness and/or insensitivity; prickling and/or tingling; burning sensation; aching pain or tightness; sharp, shooting, lancinating pain; and allodynia and/or hyperalgesia) (18). A detailed upper and lower limb neurological examination was also performed and graded using the Toronto Clinical Neuropathy Score (TCNS) (19). The examination included assessment of temperature, light touch, pinprick sensation, joint position proprioception, vibration perception, deep tendon reflexes, and motor power. The Pain Catastrophizing Scale (PCS) was used as a measure of pain-related anxiety (20).

Nerve Conduction Studies

The American Academy of Neurology and American Association of Neuromuscular & Electrodiagnostic Medicine recommendations were used to confirm the presence of DPN. The minimum case definition criteria used were an abnormality of any attribute of nerve conduction in two separate nerves, one of which was the sural nerve (21). Nerve conduction studies were performed at a stable skin temperature of 31°C and a room temperature of 24°C using a Medelec electrophysiological system using surface electrodes (Synergy; Oxford Instruments, Oxford, U.K.). A warm-water bath was used to warm cool limbs prior to testing and maintained, if necessary, using an external electric heater. The limb temperature refers to surface temperature at the point of assessment using a contact temperature probe. The following nerve attributes were measured: 1) sural sensory nerve action potentials and conduction velocities, and 2) common peroneal and tibial motor nerve distal latency, compound muscle action potential, and conduction velocity. Variables such as age, height, sex, and weight were measured and accounted for when interpreting nerve conduction results. There were 10 sural nerve (5 responders and 5 nonresponders) and 5 peroneal nerve conduction responses (3 responders and 2 nonresponders) that were not recordable.

MRI Acquisition

All MRI data were acquired at 3.0T (Ingenia; Philips Medical Systems, Best, Holland). Anatomical data were acquired using a T1-weighted magnetization-prepared

rapid acquisition gradient-echo sequence with the following parameters: repetition time 7.2 ms, echo time 3.2 ms, flip angle 8°, and voxel size 0.9 mm³, yielding isotropic spatial resolution. A 6-min resting-state functional MRI (fMRI) sequence was acquired while patients fixated on a cross using a T2*-weighted pulse sequence, with echo time of 35 ms, repetition time of 2,600 ms, in-plane pixel dimensions of 1.8 mm × 1.8 mm, and contiguous transaxial slices thickness of 4 mm orientated in the oblique axial plane parallel to the anterior commissure–posterior commissure bisection, covering the whole cerebral cortex.

MRI Analyses

Cortical Volume Assessments

Cortical reconstruction and volumetric segmentation were performed with FreeSurfer software (<https://surfer.nmr.mgh.harvard.edu>). This processing includes motion correction and averaging (22) of volumetric T1-weighted images, removal of nonbrain tissue using a hybrid watershed/surface deformation procedure (23) affine-registered to the Talairach Atlas (24,25), intensity normalization, tessellation of the gray matter–white matter boundary, automated topology correction (26,27), and surface deformation following intensity gradients to optimally place the gray/white and gray/cerebrospinal fluid borders at the location where the greatest shift in intensity defines the transition to the other tissue class (28,29). We visually inspected the original T1 image and the FreeSurfer segmented output. Inaccurate reconstruction and error correction were implemented based on workflow recommended (<https://surfer.nmr.mgh.harvard.edu/fswiki/RecommendedReconstruction>). Also, in the area of interest, we looked out for outliers in the extracted FreeSurfer data. Imaging data sets of any outliers were re-evaluated to ensure there were no segmentation errors. Cortical vertices/volumes and deep-brain nuclei volumes (in milliliters) of seven regions of interest (ROIs) were measured. The seven ROIs chosen are well-recognized brain regions involved with somatic and nonsomatic nociception. These include: primary somatosensory cortex (S1), insula cortex, cingulate gyrus, thalamus, orbital frontal cortex, amygdala, and nucleus accumbens. Volumetric data for each ROI were averaged between the two hemispheres prior to analysis being performed.

Functional Connectivity

Functional connectivity analysis was performed with the Neuroimaging Tools & Resource Collaboratory Functional Connectivity (CONN) Toolbox (30) and SPM8 (Wellcome Centre for Human Neuroimaging, London, U.K.) in MATLAB 2014a (MathWorks, Natick, MA) to generate ROI-to-ROI connectivity matrices and test hypotheses and visualize data. CONN used the CompCor strategy for spatial and temporal preprocessing to define and remove confounds in the blood oxygen level–dependent signal to prevent the impact of physiological noise factors and motion in the data (31). Fisher transformation was used to convert correlation coefficients to normally distributed

scores to enable second-level general linear model analysis (29). The correlation maps were dependent on the specific location of the seed so that functionally and anatomically heterogeneous ROIs were dissociated in order to delineate functional boundaries across the cortex (29). CONN created subject-specific ROI files for the seven ROIs and registered them to the subject space. These ROIs were used as the seeds of interest for subject-specific ROI-to-ROI connectivity analyses. Functional connectivity measures were computed between seed areas for ROI-to-ROI analysis and to create ROI-to-ROI connectivity. The CONN toolbox used a linear measure of functional connectivity between bivariate correlation and bivariate regression coefficients, with their associated multivariate measures of semipartial-correlation and multivariate-regression coefficients to calculate functional connectivity (29). After each subject had ROI-to-ROI connectivity matrices, the ROI-level analyses were evaluated through *F* or Wilks λ statistics depending on the dimensionality of the within- and between-subjects contrasts. Connectivity contrast effect size among all ROI sources was calculated alongside *t* and *F* values, uncorrected *P* values, and false discovery rate (FDR)–corrected *P* values for each specified second-level analysis. The *F* test was used to calculate the multivariate connectivity strength for each threshold. We tested the lidocaine responder versus nonresponder interaction. The significance of ROI-to-ROI connection was determined through false-positive control FDR-corrected *P* values with a χ^2 test with two-sided inferences. The CONN toolbox ROI-to-ROI analyses results are considered appropriately corrected for multiple comparisons across all brain and analysis voxels when the height voxel-level and the extent cluster-level thresholds use an analysis-wise false-positive control FDR-corrected *P* values method (29).

Statistical Analyses

Categorical variables were expressed as numbers and percentages and when compared with the use of Fisher exact or ordinal χ^2 tests as appropriate. Continuous variables were expressed as medians and interquartile ranges or as means and SDs, as appropriate, and compared using two-way between-groups ANOVA tests. Subsequent subgroup comparisons were performed using a post hoc analysis if ANOVA test was significant. The proportion of patients with the IR and NIR nociceptor phenotypes in responders versus nonresponders to intravenous lidocaine treatment was compared using χ^2 tests. Odds ratios and relative risks were calculated to examine the association between each DFNS QST parameter and treatment outcome. We also performed a secondary sensitivity analysis of sensory profiles and QST parameters between responders defined as an improvement in pain intensity score of >50% compared with nonresponders (<30% improvement). The relationships between NTSS-6 (somatic measure) and PCS (nonsomatic measure) and resting-state fMRI functional connectivity were investigated using Pearson product-moment correlation coefficient. This analysis was restricted

to the most relevant variables and averaged across both hemispheres to minimize the number of correlations performed. We chose to examine the functional connectivity of the bilateral insula and primary somatosensory cortices. Preliminary analyses were performed to ensure no violations of the assumptions of normality, linearity, and homoscedasticity. A conservative threshold of significance was chosen ($\alpha < 0.01$) for each independent variable to account for multiple correlations performed (32). We also report on the strength of the relationship (ρ) and the amount of shared variance (percentage and coefficient of determination). All tests were two-sided. Statistical analysis was carried out with SPSS version 21 software (IBM Corporation).

Data and Resource Availability

The data sets generated and/or analyzed during the study are available from the corresponding author upon reasonable request.

RESULTS

Details of demographic, clinical, and neurophysiological assessments performed are given in Tables 1 and 2. A participant flow chart is displayed in Supplementary Fig. 1.

Among responders, there was an improvement in mean pain intensity (NRS 0–10) before (8.11 [1.3]) and after (3.11 [2.0]) treatment (61.7% reduction), which took a median of 1.5 days to reach maximum effect and lasts for 6.83 (2.6) weeks (mean [SD]). Age ($P = 0.53$), pain duration ($P = 0.89$), diabetes duration ($P = 0.19$), and clinical parameters of neuropathy severity (TCNS, $P = 0.16$; NTSS-6, $P = 0.61$) were not significantly different between responders and nonresponders. Neither was there a difference in the use of concurrent neuropathic pain treatments. There was a significantly greater proportion of patients with the IR nociceptor phenotype in responders compared with nonresponders to intravenous lidocaine ($\chi^2 = 6.15$; $P = 0.02$). The odds ratio of responding to intravenous lidocaine was 8.67 times greater (95% CI 1.4–53.8) for patients with painful DPN with the IR nociceptor phenotype (relative risk 2.53 [95% CI 1.2–5.3]). Conversely, nonresponders had a significantly higher proportion of patients with the NIR nociceptor phenotype (relative risk 3.42 [95% CI 0.9–12.3]). Figure 1 depicts the forest plot of relative risk for each DFNS QST parameter for the outcome of responding to intravenous lidocaine. WUR (relative risk 2.5 [95% CI 1.5–4.0]) and dynamic mechanical allodynia (2.4 [95% CI 1.3–4.4]) had the highest relative risk

Table 1—Demographic characteristics, neurophysiological assessments, and sensory phenotype classification of study cohorts

	Responders	Nonresponders	<i>P</i>
<i>n</i>	14	15	
Age (years)	58.4 (11.1)	55.8 (10.6)	0.45
Male sex (<i>n</i> , %)	10, 71.4	7, 46.7	0.36*
Type of diabetes (type 1/2) (<i>n</i> , %)	5, 35.7	4, 26.7	0.70*
Duration of diabetes (years)	18.0 (13.5)	14.2 (10.1)	0.19
Duration of pain (years)	8.92 (7.2)	7.46 (8.1)	0.85
BMI (kg/m ²)	33.9 (9.2)	30.9 (5.8)	0.32
HbA _{1c} (mmol/mol)	68.8 (16.1)	70.3 (23.5)	0.91
HbA _{1c} (%)	8.4 (1.5)	8.6 (2.1)	0.91
NTSS-6 score	15.7 (3.3)	14.7 (5.0)	0.61
TCNS	32.5 (10.6)	25.6 (14.4)	0.25
Sural			
Conduction velocity (m/s)	36.2 (3.3)	30.6 (15.4)	0.52
Amplitude (mAmp)	2.8 (2.9)	3.4 (6.3)	0.77
Common peroneal nerve			
Conduction velocity (m/s)	36.7 (6.2)	41.2 (9.9)	0.27
Amplitude (mAmp)	1.8 (1.6)	1.2 (1.8)	0.43
Distal latency (ms)	4.5 (3.0)	5.1 (2.9)	0.60
Pain phenotype (<i>n</i> , %)			
IR nociceptor	8, 57.2	2, 13.3	0.02*
NIR nociceptor	6, 42.9	13, 86.7	
Medications (<i>n</i>)			
Pregabalin	7	6	1.00*
Duloxetine	6	3	0.37*
Amitriptyline	1	1	1.00*
Opiates	7	5	0.65*
Other	0	2	0.47*

Data are mean (SD) unless otherwise indicated. Statistically significant results (i.e., $P < 0.05$) appear in boldface type. * P values for χ^2 test.

Table 2—Results of QST using the DFNS protocol

	Responders	Nonresponders	<i>P</i>
CDT (°C)	−20.8 (11.4)	−16.1 (12.3)	0.30
z score	−2.83 (0.7)	−2.87 (0.5)	
WDT (°C)	16.1 (2.3)	14.7 (2.7)	0.21
z score	−2.02 (0.4)	−1.94 (0.3)	
TSL (°C)	36.2 (18.0)	35.8 (10.4)	0.95
z score	−2.68 (0.8)	−2.35 (0.5)	
CPT (°C)	2.37 (7.0)	5.99 (9.3)	0.30
z score	−0.80 (0.8)	−0.47 (0.9)	
HPT (°C)	49.9 (0.2)	48.8 (1.2)	0.005
z score	−1.57 (0.3)	−1.19 (0.4)	
PPT	585.9 (592.3)	664.1 (502.6)	0.75
z score	−1.18 (1.9)	−0.61 (2.2)	
MPT	493.0 (270.0)	441.7 (315.2)	0.68
z score	−2.16 (1.2)	−1.43 (1.6)	
MPS	4.89 (12.7)	8.89 (10.9)	0.49
z score	−0.42 (2.0)	−0.51 (1.8)	
MDT	344.2 (321.8)	377.4 (365.7)	0.82
z score	−3.68 (1.5)	−3.73 (1.1)	
VDT	3.50 (2.5)	3.29 (2.4)	0.83
z score	−3.36 (2.5)	−3.51 (2.3)	
WUR (<i>n</i> , %)			
Present	4, 28.6	0, 0	0.04*
Absent	10, 71.4	15, 100	
PHS (<i>n</i> , %)			
Present	4, 28.6	7, 46.7	0.45*
Absent	10, 71.4	8, 53.3	
DMS (<i>n</i> , %)			
Present	6, 42.9	1, 6.7	0.03*
Absent	8, 57.1	14, 93.3	

Data are mean (SD) unless otherwise indicated. Statistically significant results (i.e., $P < 0.05$) appear in boldface type. CDT, cold detection threshold; CPT, cold pain threshold; DMS, dynamic mechanical sensitivity; HPT, heat pain threshold; MDT, mechanical detection threshold; MPS, mechanical pain sensitivity; MPT, mechanical pain threshold; PHS, paradoxical heat sensation; TSL, thermal sensory limen; VDT, vibration detection threshold; WDT, warm detection threshold. * P values for χ^2 test.

compared with the other DFNS QST parameters. There were no significant differences in thermal, mechanical, or vibration detection thresholds between responders and nonresponders to treatment (Table 2 and Supplementary Figs. 2–4). Next, we performed a secondary sensitivity analysis by defining responders as patients who report at least a 50% reduction ($n = 12$) in pain intensity score. The difference in the proportions of patients with the IR nociceptor phenotype remained significant ($\chi^2 = 4.3$; $P = 0.04$). There was, however, no significant difference in dynamic mechanical sensitivity and WUR QST parameters.

MRI data from 21 patients (11 responders and 10 nonresponders) were obtained for analysis (3 had claustrophobia, 4 had unusable scans, and 1 failed to attend MRI visit). Nonresponders to intravenous lidocaine had significantly lower mean S1 cortical volumes (7.1 [1.0] mL; ANOVA $P = 0.02$) (Fig. 2) and mean number of vertices (5.4×10^3 [0.6×10^3]; ANOVA $P = 0.02$) compared with responders (volume: 8.3 [0.9] mL; vertices: 6.2×10^3 [0.5×10^3]) and healthy control subjects (volume: 8.1

[0.9] mL; vertices: 6.0×10^3 [0.6×10^3]). There was no significant difference in S1 cortical volumes or vertices between responders and healthy control subjects. Thalamic (responders vs. nonresponders: 6.7×10^3 [1.0×10^3] vs. 6.5×10^3 [0.7×10^3]; $P = 0.37$), insula (6.0×10^3 [0.6×10^3] vs. 5.9×10^3 [0.7×10^3]; $P = 0.87$) and other subcortical and cortical volumes were not significantly different between the study groups. There was significantly greater resting-state functional connectivity in lidocaine responders between the insula cortex ($F[4]$ [13] = 10.33; P -FDR = 0.01) and the orbital frontal cortex ($t[20] = 3.88$; P -FDR = 0.02) and amygdala ($t[20] = 3.65$; P -FDR = 0.02) on the right (Fig. 3). Similarly, on the left, there was significantly greater functional connectivity between the insula cortex ($F[4]$ [13] = 6.46; P -FDR = 0.04) and the anterior cingulate gyrus ($t[20] = 4.04$; P -FDR = 0.01), orbital frontal cortex ($t[20] = 3.90$; P -FDR = 0.01), and nucleus accumbens ($t[20] = 3.50$; P -FDR = 0.02) in responders to intravenous lidocaine treatment. Compared with HVs, nonresponders had significantly reduced S1-motor cortical functional connectivity ($t[20] = 5.58$; P -FDR = 0.04).

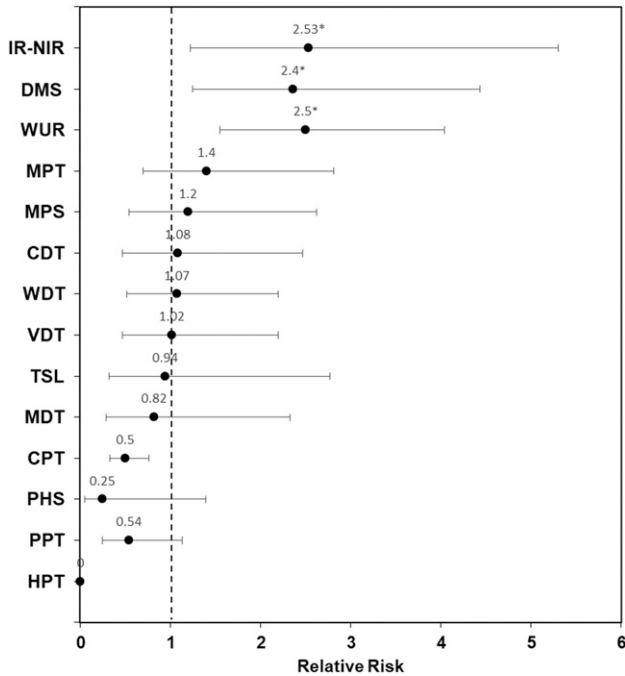


Figure 1—Forest plot of the odds ratio of each QST parameter derived from the DFNS for the outcome of responder to intravenous lidocaine treatment. * $P < 0.05$. CDT, cold detection threshold; CPT, cold pain threshold; DMS, dynamic mechanical sensitivity; HPT, heat pain threshold; MDT, mechanical detection threshold; MPS, mechanical pain sensitivity; MPT, mechanical pain threshold; PHS, paradoxical heat sensation; TSL, thermal sensory limen; VDT, vibration detection threshold; WDT, warm detection threshold.

In addition, there was also reduced thalamic–paracingulate cortical functional connectivity in nonresponders compared with HVs ($t[20] = 5.77$; $P\text{-FDR} = 0.02$). There was no significant difference in functional connectivity between HVs and responders.

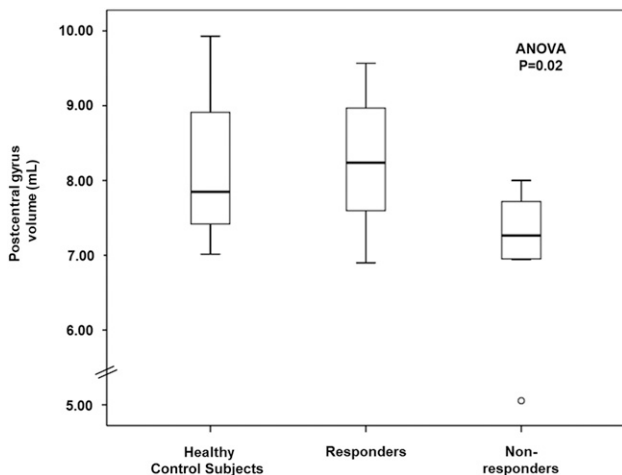


Figure 2—Box-and-whisker plots depicting median (upper and lower quartiles) posterior central gyrus cortical volume (in milliliters) of study cohorts.

Finally, after adjusting for multiple comparisons, there was a nonsignificant positive correlation between the insula–postcentral cortex ($r = 0.53$; 28.1% shared variance; $P = 0.04$) average functional connectivity and total PCS. Postcentral cortex–orbital frontal cortex ($r = -0.51$; 26%; $P = 0.01$) averaged functional connectivity was negatively correlated with NTSS-6 pain scores (Supplementary Fig. 5). There was a nonsignificant negative correlation between postcentral cortex–thalamus ($r = -0.48$; 23.0%; $P = 0.02$) average functional connectivity with NTSS-6 pain scores.

DISCUSSION

Using detailed QST (DFNS protocol), we sought to identify key phenotypic differences in sensory profiling associated with intravenous lidocaine treatment response in patients with severe, intractable painful DPN. The main study finding was that patients with the IR nociceptor phenotype were more likely to respond to intravenous lidocaine treatment compared with the NIR nociceptor phenotype. As in previous studies, we found that the sensory loss phenotype or deafferentation is the predominant feature of patients with painful DPN (3). Those with the IR nociceptor phenotype demonstrated signs of sensory gain, often in conjunction with hyposensitivity. Dynamic mechanical (brush-evoked) allodynia and wind-up were the only evoked “gain-of-function” parameters that informed response to treatment, with a higher prevalence in responders compared with nonresponders. The presence of these sensory gain parameters would suggest aberrant central processing with hyperexcitable neurons generating ectopic impulses and amplification of afferent sensory inputs (33). This hyperexcitability is driven by abnormal sodium channel regulation that triggers and maintains central sensitization (34). Hence, membrane-stabilizing sodium channel ligands such as lidocaine, which selectively inhibits this hyperexcitability, may be more efficacious in patients with this phenotype.

Our findings conform with other studies of intravenous lidocaine treatment in neuropathic pain from different etiologies. In a randomized, double-blind, placebo-controlled trial in 22 patients with postherpetic neuralgia and traumatic nerve injury, Attal et al. (35) found that mechanical allodynia predicted the response to intravenous lidocaine treatment. In a similar cohort of patients with neuropathic pain secondary to traumatic nerve injury or postherpetic neuralgia, Demant et al. (36) examined for phenotype difference in treatment effect with a lidocaine 5% patch in a randomized double-blind, crossover study. There was no significant interaction between treatment effect and phenotype, although there was a significant interaction with paroxysmal pain and deep aching pain. They conclude that the lidocaine 5% patch may be most efficacious in patients with the IR nociceptor phenotype, but the study was hampered by low statistical power (36). Our study is one of only a handful of studies that have attempted to systematically determine the value of a mechanism-based approach in painful DPN. Other examples include a randomized,

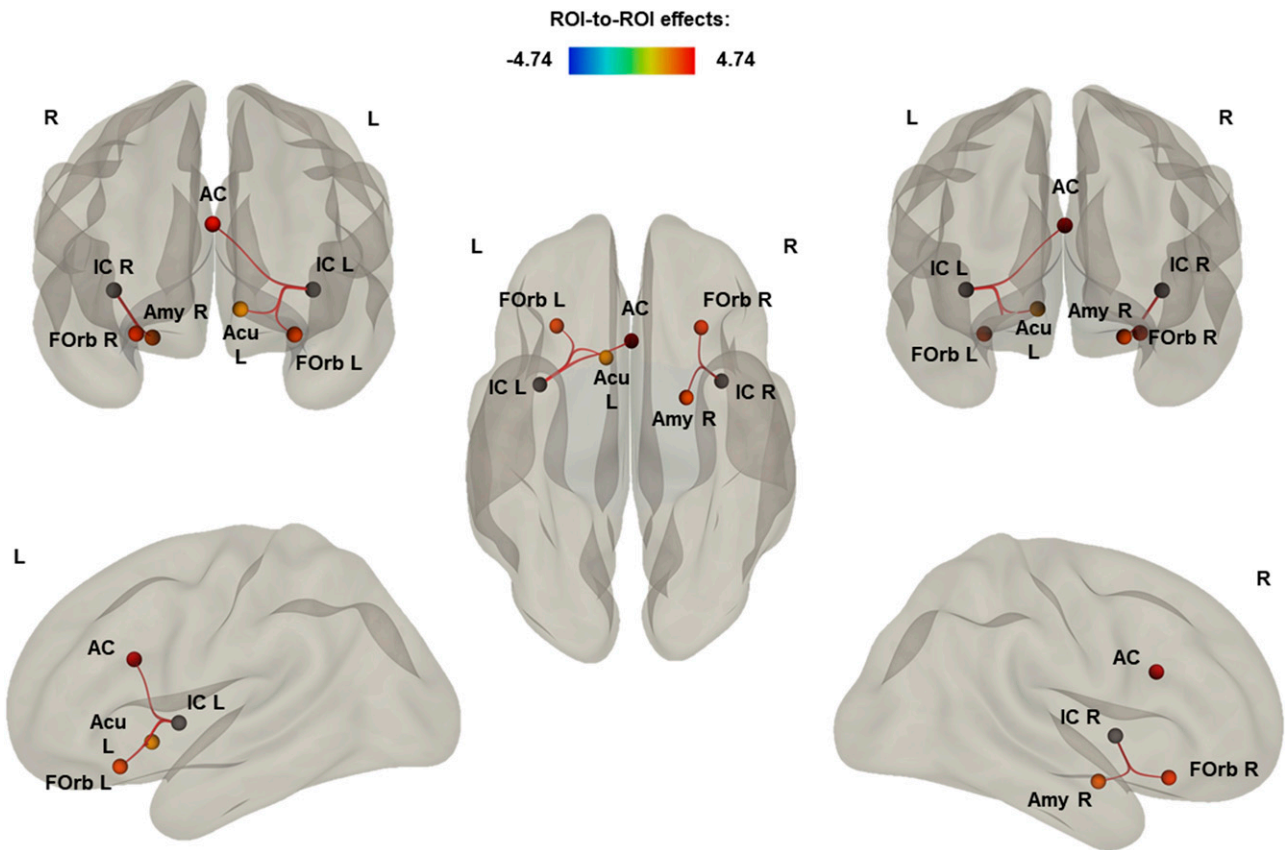


Figure 3—Anterior, posterior, left, right, and superior view of bilateral insular cortices resting-state functional connectivity in responders and nonresponders to intravenous lidocaine treatment. Red to blue = positive to negative z scores. AC, anterior cingulate gyrus; Acu, nucleus accumbens; Amy, amygdala; FOrb, orbital frontal cortex; IC, insula cortex; L, left; R, right.

placebo-controlled study by Campbell et al. (37) using topical clonidine in 179 patients with painful DPN. In this study, sensory profiling was performed using the capsaicin challenge test, and the post hoc analysis demonstrated a significant reduction in pain in the subgroup of patients with increased spontaneous pain following cutaneous capsaicin administration, indicating the presence of functioning and sensitized nociceptors. Bouhassira et al. (38) published post hoc analysis data of treatment response based on sensory profiling using the Neuropathic Pain Symptom Inventory questionnaire from the COMBO-DN study. This study examined the effect of high-dose duloxetine or pregabalin monotherapy versus a combination of pregabalin and duloxetine in painful DPN. They showed greater improvement in the dimensions of “pressing pain” and “evoked pain” with the addition of pregabalin 300 mg to duloxetine 60 mg treatment, whereas there was a greater improvement in the dimension “paraesthesia/dysesthesia” when duloxetine was increased from 60 to 120 mg a day. Taken together, these studies support the notion that a mechanism-based approach to pain management may be feasible in painful DPN. However, in an elegant mechanistic study, Haroutounian et al. (39) examined 14 patients with neuropathic pain of mixed etiology (unilateral foot pain from nerve injury [$n = 7$] and distal polyneuropathy

[$n = 7$]) to determine the contribution of primary afferent input in maintaining peripheral neuropathic pain. Each patient underwent ultrasound-guided peripheral nerve block with lidocaine and intravenous lidocaine infusion in randomized order. They found that peripheral afferent input was critical for maintaining neuropathic pain but improvement in evoked hypersensitivity was not related to improvements in spontaneous pain intensity. In our study, we did not repeat QST following intravenous lidocaine administration to determine its effect on individual sensory parameters. Hence, further definitive evidence is now required in the form of a prospective, double-blind randomized control trial in which patients are stratified into sensory phenotypes prior to randomization. Proof-of-concept for this approach has been provided by the recent oxcarbazepine trial by Demant et al. (4), but it only included a small subset (10.8%) of patients with painful DPN.

In our exploratory neuroimaging study, we found significantly lower S1 cortical volumes and functional connectivity in nonresponders. We have previously reported reduction in S1 cortical volumes in patients with painful DPN with the painful insensate phenotype (9). One common trait shared by both subtypes is the absence of hyperalgesia or evoked/contact hypersensitivity (e.g., allodynia). Therefore, we postulate that absence of this form of

pathological peripheral nociceptive stimulus may lead to a greater reduction in S1 cortical volume in painful DPN. In addition, responders to intravenous lidocaine treatment have significantly greater functional connectivity between the insula cortex and corticolimbic system (orbital frontal cortex, amygdala, cingulate cortex, and nucleus accumbens). The insula (40) cortex plays a pivotal role in processing the emotion and cognitive dimensions of the chronic pain experience. The corticolimbic circuits have also long been implicated in reward, decision making, and fear learning (41). Hence, our findings suggest that this network may have a role in determining treatment response in painful DPN. This is supported by significant correlations between functional connectivity of the primary somatosensory cortex and somatic measures of pain (NTSS-6). Although the relationship between the functional connectivity of the insula cortex with PCS (nonsomatic measure) was not significant after adjustment for multiple comparisons, there was a respectable amount of shared variance and a modest relationship between the two variables. Nonresponders also demonstrated reduced thalamic–paracingulate cortical functional connectivity compared with HVs. The paracingulate, which is part of the medial prefrontal cortex, is an important region involved in executive function (e.g., processing working memory and decision making). It is also involved in pain processing, which is dependent on its connections to the thalamus. Sensory stimulus is transformed in the prefrontal cortex into a perceptual signal, which is then used to control the flow of sensory stimuli at their entrance to the CNS (dorsal horn) (42). This antinociceptive effect is mediated by connections to the periaqueductal gray, resulting in the modulation of pain (top-down inhibition). Hence, reduction in thalamic–paracingulate cortical functional connectivity in nonresponders indicates abnormal descending pain modulation. There was no significant difference in functional connectivity between HVs and responders to intravenous lidocaine treatment. Resting-state fMRI would not be the most appropriate magnetic resonance (MR) modality to examine alterations in regional functional connectivity in responders, as they were characterized by presence of dynamic mechanical allodynia, an evoked pain response. A more suitable experiment would be an event-related or boxcar fMRI experiment in which allodynia is reproduced during fMRI acquisition. Similar experiments have been performed in HVs (using the capsaicin-induced hyperalgesia model) and in other chronic pain conditions (43–49).

This study has some limitations, including: 1) this was an open-labeled retrospective study. However, the neurophysiological and MR assessments performed were objective, and it provides preliminary evidence for a mechanism-based approach to pain management in painful DPN. Nevertheless, as the reporting of pain responses is not objective, the next important step is a blinded, randomized control trial in which patients are stratified into subgroups at baseline according to their phenotype based on sensory

profiling and/or neuroimaging. This will establish the effectiveness of an individualized mechanism-based approach to therapy in painful DPN. 2) There was a drop (27%) in the number of patients with completed/usable MR data. The main reasons for this were claustrophobia or failing to attend the MR study visit. There was no significant difference in mean age, duration of pain, HbA_{1c}, and NTSS-6 or DN4 scores between patients with and without MR data. All subjects were well characterized, and the study provides a novel insight into the peripheral and central mechanisms of treatment response in painful DPN. Furthermore, the MRI results obtained are robust ($P < 0.05$), even after correction for multiple comparisons using an FDR method. 3) We examined patients with severe intractable pain, resistant to conventional neuropathic pain treatments, who often pose a challenge to manage. Hence, the findings of this study may not be generalizable to a wider population of patients with painful DPN. More data are needed to determine if intravenous lidocaine can provide safe and effective pain relief in this needy group of patients and if adopting a stratified approach to treatment selection reduces patient inconvenience and overall cost of treatment. 4) This proof-of-concept study has a small sample size, which limits our ability to correct for potential confounders and test alternative hypotheses (e.g., differences between sexes and diabetes status). Further studies are now needed not only to confirm the findings of this study but also to inform the approach toward embedding a personalized medicine approach into mainstream care of patients with painful DPN.

In summary, considerable progress has been made in the last decade toward a mechanism-based approach to the management of painful DPN. This study, to the best of our knowledge, is the first exploratory study to assess both peripheral and central mechanisms of treatment response in painful DPN. In our select group of patients, we have demonstrated that QST could be used to identify those with the IR nociceptor phenotype, which may inform their response to intravenous lidocaine treatment. Moreover, within the CNS, key sensorimotor areas showed decreased gray matter density (S1 cortex) and reduced functional connectivity (insula) that may also inform treatment response. In the context of a wider cohort of painful DPN, our study population may only comprise a small subset of patients. Nevertheless, these individuals suffer significant pain-related morbidity, comprise a sizeable population in secondary/tertiary care clinics, and are most in need of effective/efficient pain management. In the future, we want to conduct a large prospective observational cohort study with more detailed phenotyping of patients including skin biopsies, molecular biomarkers of pain, genotyping, and more detailed brain-imaging paradigms to determine the most reliable predictor of treatment response in painful DPN.

Acknowledgments. The authors thank the radiographers at the University of Sheffield Academic Department of Magnetic Resonance Imaging for their hard

work, skills, and contributions. The authors also thank the study volunteers who spent considerable time participating in this study.

Funding. This study was supported by the European Foundation for the Study of Diabetes (Microvascular Complications Project Grant), the National Institute of Health Research Efficacy and Mechanism Evaluation Programme (NIHR129921), and the University of Sheffield, Health Education England, Knowledge Exchange fund.

Duality of Interest. No potential conflicts of interest relevant to this article were reported.

Author Contributions. I.D.W. undertook planning of MR experiments and reviewed and revised the manuscript. K.T. analyzed MR cortical thickness and resting-state fMRI data. F.H.-G., M.A., P.S., and G.S. certified in DFNS QST assessments and undertook clinical and neurophysiological assessments. A.K. collected and collated data on clinical and neurophysiological assessments. S.T. reviewed and revised the manuscript. D.S. recruited participants, undertook clinical and neurophysiological assessments, researched and analyzed clinical and MR data, and wrote the manuscript. D.S. is the guarantor of this work and, as such, had full access to all the data in the study and takes responsibility for the integrity of the data and the accuracy of the data analysis.

References

- Albers JW, Pop-Busui R. Diabetic neuropathy: mechanisms, emerging treatments, and subtypes. *Curr Neurol Neurosci Rep* 2014;14:473
- Finnerup NB, Sindrup SH, Jensen TS. The evidence for pharmacological treatment of neuropathic pain. *Pain* 2010;150:573–581
- Themistocleous AC, Ramirez JD, Shillo PR, et al. The Pain in Neuropathy Study (PINS): a cross-sectional observational study determining the somatosensory phenotype of painful and painless diabetic neuropathy. *Pain* 2016;157:1132–1145
- Demant DT, Lund K, Vollert J, et al. The effect of oxcarbazepine in peripheral neuropathic pain depends on pain phenotype: a randomised, double-blind, placebo-controlled phenotype-stratified study. *Pain* 2014;155:2263–2273
- Challapalli V, Tremont-Lukats IW, McNicol ED, Lau J, Carr DB. Systemic administration of local anesthetic agents to relieve neuropathic pain. *Cochrane Database Syst Rev* 2005;4:CD003345.
- Bach FW, Jensen TS, Kastrup J, Stigsby B, Dejgård A. The effect of intravenous lidocaine on nociceptive processing in diabetic neuropathy. *Pain* 1990;40:29–34
- Tesfaye S, Vileikyte L, Rayman G, et al.; Toronto Expert Panel on Diabetic Neuropathy. Painful diabetic peripheral neuropathy: consensus recommendations on diagnosis, assessment and management. *Diabetes Metab Res Rev* 2011;27:629–638
- Challapalli V, Tremont-Lukats IW, McNicol ED, Lau J, Carr DB. Systemic administration of local anesthetic agents to relieve neuropathic pain. *Cochrane Database Syst Rev* 2005;2005:CD003345
- Sheets PL, Jarecki BW, Cummins TR. Lidocaine reduces the transition to slow inactivation in Na(v)1.7 voltage-gated sodium channels. *Br J Pharmacol* 2011;164:719–730
- Jasmin L, Kohan L, Franssen M, Janni G, Goff JR. The cold plate as a test of nociceptive behaviors: description and application to the study of chronic neuropathic and inflammatory pain models. *Pain* 1998;75:367–382
- Chaplan SR, Bach FW, Shafer SL, Yaksh TL. Prolonged alleviation of tactile allodynia by intravenous lidocaine in neuropathic rats. *Anesthesiology* 1995;83:775–785
- Selvarajah D, Wilkinson ID, Fang F, et al. Structural and functional abnormalities of the primary somatosensory cortex in diabetic peripheral neuropathy: a multimodal MRI study. *Diabetes* 2019;68:796–806
- Bouhassira D, Attal N, Alchaar H, et al. Comparison of pain syndromes associated with nervous or somatic lesions and development of a new neuropathic pain diagnostic questionnaire (DN4). *Pain* 2005;114:29–36
- Dworkin RH, Turk DC, Peirce-Sandner S, et al. Considerations for improving assay sensitivity in chronic pain clinical trials: IMMPACT recommendations. *Pain* 2012;153:1148–1158
- Rolke R, Magerl W, Campbell KA, et al. Quantitative sensory testing: a comprehensive protocol for clinical trials. *Eur J Pain* 2006;10:77–88
- Magerl W, Krumova EK, Baron R, Tölle T, Treede RD, Maier C. Reference data for quantitative sensory testing (QST): refined stratification for age and a novel method for statistical comparison of group data. *Pain* 2010;151:598–605
- Vollert J, Maier C, Attal N, et al. Stratifying patients with peripheral neuropathic pain based on sensory profiles: algorithm and sample size recommendations. *Pain* 2017;158:1446–1455
- Bastyr EJ III, Price KL, Bril V; MBBQ Study Group. Development and validity testing of the neuropathy total symptom score-6: questionnaire for the study of sensory symptoms of diabetic peripheral neuropathy. *Clin Ther* 2005;27:1278–1294
- Bril V, Tomioka S, Buchanan RA, Perkins BA; mTCNS Study Group. Reliability and validity of the modified Toronto Clinical Neuropathy Score in diabetic sensorimotor polyneuropathy. *Diabet Med* 2009;26:240–246
- Sullivan MJ, Bishop SR, Pivik J. The pain catastrophizing scale: development and validation. *Psychol Assess* 1995;7:524–532
- England JD, Gronseth GS, Franklin G, et al.; American Academy of Neurology; American Association of Electrodiagnostic Medicine; American Academy of Physical Medicine and Rehabilitation. Distal symmetric polyneuropathy: a definition for clinical research: report of the American Academy of Neurology, the American Association of Electrodiagnostic Medicine, and the American Academy of Physical Medicine and Rehabilitation. *Neurology* 2005;64:199–207
- Reuter M, Rosas HD, Fischl B. Highly accurate inverse consistent registration: a robust approach. *Neuroimage* 2010;53:1181–1196
- Ségonne F, Dale AM, Busa E, et al. A hybrid approach to the skull stripping problem in MRI. *Neuroimage* 2004;22:1060–1075
- Fischl B, Salat DH, van der Kouwe AJ, et al. Sequence-independent segmentation of magnetic resonance images. *Neuroimage* 2004;23(Suppl. 1):S69–S84
- Fischl B, Salat DH, Busa E, et al. Whole brain segmentation: automated labeling of neuroanatomical structures in the human brain. *Neuron* 2002;33:341–355
- Ségonne F, Pacheco J, Fischl B. Geometrically accurate topology-correction of cortical surfaces using nonseparating loops. *IEEE Trans Med Imaging* 2007;26:518–529
- Fischl B, Liu A, Dale AM. Automated manifold surgery: constructing geometrically accurate and topologically correct models of the human cerebral cortex. *IEEE Trans Med Imaging* 2001;20:70–80
- Fischl B, Dale AM. Measuring the thickness of the human cerebral cortex from magnetic resonance images. *Proc Natl Acad Sci U S A* 2000;97:11050–11055
- Dale AM, Fischl B, Sereno MI. Cortical surface-based analysis. I. Segmentation and surface reconstruction. *Neuroimage* 1999;9:179–194
- Dib-Hajj SD, Cummins TR, Black JA, Waxman SG. Sodium channels in normal and pathological pain. *Annu Rev Neurosci* 2010;33:325–347
- Whitfield-Gabrieli S, Nieto-Castanon A. Conn: a functional connectivity toolbox for correlated and anticorrelated brain networks. *Brain Connect* 2012;2:125–141
- Behzadi Y, Restom K, Liu J, Liu TT. A component based noise correction method (CompCor) for BOLD and perfusion based fMRI. *Neuroimage* 2007;37:90–101
- Curtin F, Schulz P. Multiple correlations and Bonferroni's correction. *Biol Psychiatry* 1998;44:775–777
- Jensen TS, Finnerup NB. Allodynia and hyperalgesia in neuropathic pain: clinical manifestations and mechanisms. *Lancet Neurol* 2014;13:924–935
- Attal N, Rouaud J, Brasseur L, Chauvin M, Bouhassira D. Systemic lidocaine in pain due to peripheral nerve injury and predictors of response. *Neurology* 2004;62:218–225
- Demant DT, Lund K, Finnerup NB, et al. Pain relief with lidocaine 5% patch in localized peripheral neuropathic pain in relation to pain phenotype: a randomised, double-blind, and placebo-controlled, phenotype panel study. *Pain* 2015;156:2234–2244
- Campbell CM, Kipnes MS, Stouch BC, et al. Randomized control trial of topical clonidine for treatment of painful diabetic neuropathy. *Pain* 2012;153:1815–1823

38. Bouhassira D, Wilhelm S, Schacht A, et al. Neuropathic pain phenotyping as a predictor of treatment response in painful diabetic neuropathy: data from the randomized, double-blind, COMBO-DN study. *Pain* 2014;155:2171–2179
39. Haroutounian S, Nikolajsen L, Bendtsen TF, et al. Primary afferent input critical for maintaining spontaneous pain in peripheral neuropathy. *Pain* 2014;155:1272–1279
40. Lu C, Yang T, Zhao H, et al. Insular cortex is critical for the perception, modulation, and chronification of pain. *Neurosci Bull* 2016;32:191–201
41. Taylor AMW. Corticolimbic circuitry in the modulation of chronic pain and substance abuse. *Prog Neuropsychopharmacol Biol Psychiatry* 2018;87:263–268
42. Jahn A, Nee DE, Alexander WH, Brown JW. Distinct regions within medial prefrontal cortex process pain and cognition. *J Neurosci* 2016;36:12385–12392
43. Iannetti GD, Zambreanu L, Wise RG, et al. Pharmacological modulation of pain-related brain activity during normal and central sensitization states in humans. *Proc Natl Acad Sci U S A* 2005;102:18195–18200
44. Maihöfner C, Handwerker HO. Differential coding of hyperalgesia in the human brain: a functional MRI study. *Neuroimage* 2005;28:996–1006
45. Rempe T, Wolff S, Riedel C, et al. Spinal and supraspinal processing of thermal stimuli: an fMRI study. *J Magn Reson Imaging* 2015;41:1046–1055
46. Schenk LA, Sprenger C, Geuter S, Büchel C. Expectation requires treatment to boost pain relief: an fMRI study. *Pain* 2014;155:150–157
47. Shenoy R, Roberts K, Papadaki A, et al. Functional MRI brain imaging studies using the Contact Heat Evoked Potential Stimulator (CHEPS) in a human volunteer topical capsaicin pain model. *J Pain Res* 2011;4:365–371
48. Wiech K, Seymour B, Kalisch R, et al. Modulation of pain processing in hyperalgesia by cognitive demand. *Neuroimage* 2005;27:59–69
49. Mainero C, Zhang W-T, Kumar A, Rosen BR, Sorensen AG. Mapping the spinal and supraspinal pathways of dynamic mechanical allodynia in the human trigeminal system using cardiac-gated fMRI. *Neuroimage* 2007;35:1201–1210